Enhancement of the Curie temperature of the amorphous intergranular phase in Sm–Fe–Ga–C nanocomposite permanent magnetic materials

2003 J. Phys.: Condens. Matter 15 267

(http://iopscience.iop.org/0953-8984/15/2/326)

INSTITUTE OF PHYSICS PUBLISHING JOURNAL OF PHYSICS: CONDENSED MATTER

J. Phys.: Condens. Matter **15** (2003) 267–274 PII: S0953-8984(03)35127-6

Enhancement of the Curie temperature of the amorphous intergranular phase in Sm–Fe–Ga–C nanocomposite permanent magnetic materials

Zhao-hua Cheng[1,2,4], **Jun-xian Zhang**[3], **H Kronmüller**[3], **R A Dunlap**[2] **and Bao-gen Shen**[1]

[1] State Key Laboratory of Magnetism, Institute of Physics and Centre of Condensed Matter Physics, Chinese Academy of Sciences, Beijing 100080, People's Republic of China
[2] Department of Physics, Dalhousie University, Halifax, NS B3H 3J5, Canada
[3] Max-Planck-Institut für Metallforschung, Heisenbergstraße 1, 70569 Stuttgart, Germany

E-mail: zhcheng@g203.iphy.ac.cn

Received 21 March 2002, in final form 28 November 2002
Published 20 December 2002
Online at stacks.iop.org/JPhysCM/15/267

Abstract

The magnetic properties of the nanocomposite permanent magnetic materials Sm–Fe–Ga–C have been investigated. As-quenched $Sm_2Fe_{18}Ga_2C_{2.2}$ samples prepared with a substrate velocity $v_s = 18.5$ and 19.5 m s^{-1} contain some amorphous intergranular phase, together with $Sm_2Fe_{15}Ga_2C_{2.2}$ (Th_2Zn_{17}-type structure) and α-Fe. On the basis of the compositional dependence of the Curie temperature in $Sm_2Fe_{15+x}Ga_2C_{2.2}$ amorphous ribbons, an enhancement of the Curie temperature of the amorphous intergranular phase (aip) was found in nanocomposite alloys with respect to amorphous ribbons of the same composition. ^{57}Fe magnetic hyperfine field distributions for the amorphous intergranular amorphous phase are narrower than those for the amorphous ribbon. No difference was found in average hyperfine field, and hence in Fe magnetic moment, within the experimental error. We also excluded the effect of compositional difference on Curie temperature. The enhancement of the Curie temperature is thus concluded to originate from the penetration of the molecular field of crystallized magnetic phases into the amorphous intergranular region. Finally, a theoretical model was proposed to explain the mechanism of 'extra' enhancement of the Curie temperature.

It is well known that nanoscale magnetic materials can exhibit significantly different magnetic properties to the corresponding bulk materials if their grain sizes are comparable with their exchange-coupling length. For example, nanocomposite permanent magnets composed

[4] Address for correspondence: State Key Laboratory of Magnetism, Institute of Physics, Chinese Academy of Sciences, PO Box 603, Beijing 100080, People's Republic of China.

of magnetically hard and magnetically soft phases show a significant enhancement of remanence [1–4]. In our previous work, nanocomposite permanent magnetic materials consisting of $Sm_2Fe_{15}Ga_2C_{2.2}$ (Th_2Zn_{17}-type structure) and α-Fe were successfully synthesized by direct melt-spinning [5]. The relationship between magnetic properties and microstructure was investigated as well. It was found that some aip coexists with $Sm_2Fe_{15}Ga_2C_{2.2}$ and α-Fe in as-quenched samples prepared with substrate velocities of $v_s = 18.5$ and 19.5 m s^{-1}. According to the temperature dependence of the magnetization curves $M(T)$, the Curie temperatures of the aips in the samples quenched at 18.5 and 19.5 m s^{-1} are about 42 and 38 K higher, respectively, than those of completely amorphous ribbons with the same composition. Since the Curie temperature of Fe-rich amorphous alloys is mainly determined by the exchange-coupling interaction between the nearest-neighbour Fe–Fe atoms, and the Mössbauer effect can be used to detect the nearest-neighbour environment of Fe nuclei, the mechanism of Curie temperature enhancement has been investigated by means of Mössbauer spectra. The contributions of the Fe magnetic moment difference, compositional difference, and molecular field penetration into the aip to the enhancement in the Curie temperature have been discussed.

Alloys with composition $Sm_2Fe_{15+x}Ga_2C_{2.2}$ ($x = 0$, 1.5, 3.0, and 4.5) were prepared by arc melting. As-quenched ribbons with a width of about 2.5 mm and a thickness of 25–35 μm were prepared by melt-spinning in a highly pure helium atmosphere at the substrate velocities $v_s = 18.5$–35.0 m s^{-1}. The microstructural properties, such as the crystallite size and its distribution, were investigated by using a transmission electron microscope (TEM). Thermomagnetic curves were measured in a field of 1 kOe from 300 to 700 K. Room temperature ^{57}Fe Mössbauer spectra were collected using a Wissel System II constant-acceleration spectrometer with a Pd^{57}Co source. The velocity scale was calibrated using α-Fe foil.

Figures 1(a) and (b) present the TEM micrograph and the selected-area electron diffraction pattern of the sample quenched at 18.5 m s^{-1}, respectively. TEM observation shows that the larger crystallites correspond to the major phase $Sm_2Fe_{15}Ga_2C_{2.2}$ while the minor phase α-Fe has smaller crystallites and is located at the grain boundaries between areas of major phase. The TEM micrographs and electron diffraction patterns for different areas are found to be uniform, which suggests a homogeneous chemical composition for the as-quenched ribbons. No obviously preferential orientation of the crystallites is observed from either x-ray diffraction or electron diffraction patterns. The average crystallites diameters of $Sm_2Fe_{15}Ga_2C_x$ and a-Fe are 60–70 and 20–30 nm, respectively. Some amorphous phases exist in the samples quenched at 18.5 and 19.5 m s^{-1}. In order to confirm the TEM observation, thermomagnetic curves of as-quenched $Sm_2Fe_{18}Ga_2C_{2.2}$ ribbons at various substrate velocities were obtained in a magnetic field of 1 kOe, and these are presented in figure 2. The temperature dependence of the magnetization for the sample quenched at 35.0 m s^{-1} exhibits a single magnetic amorphous phase behaviour. After decreasing to nearly 0 emu g^{-1}, the magnetization increases with further increasing temperature. A further increase in magnetization implies that crystallization of the amorphous state begins to occur at around 600 K. Therefore, the heating and cooling M–T curves are found to be irreversible. The Curie temperature of the amorphous alloy can be estimated from the intersection point of the steepest tangent of $M(T)$ with the T-axis. The error bar on the T_C-value obtained by this method is within ± 5 K after calibration using a Ni standard sample. For the samples quenched at 18.5 and 19.5 m s^{-1}, the M–T curves show two magnetic phase transitions in the temperature range of 300–700 K. The lower Curie temperature, which corresponds to the aip, can be estimated from the intersection point of the steepest tangent of the $M(T)$ curves with the magnetization curves of the crystallized phase extrapolated down to temperatures below the Curie temperature of the aip. The magnetic phase

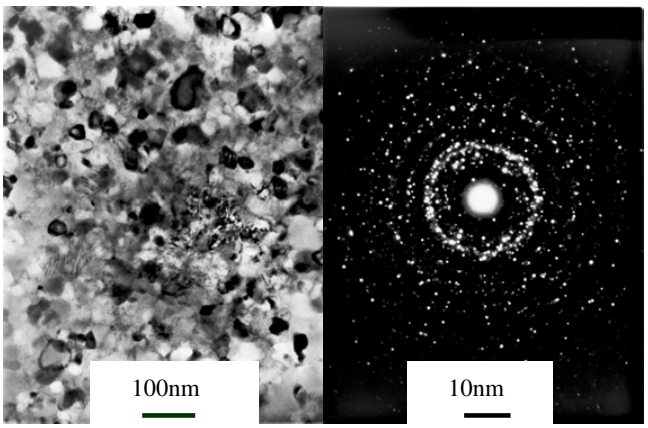

Figure 1. A TEM micrograph (a) and a selected-area electron pattern for the sample quenched at 18.5 m s^{-1} (b).

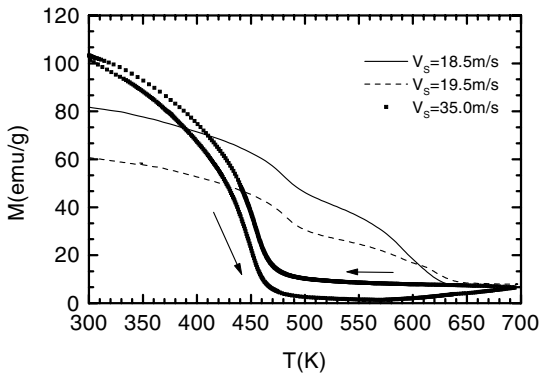

Figure 2. Thermomagnetic curves of as-quenched $Sm_2Fe_{18}Ga_2C_{2.2}$ samples prepared with different substrate velocities in a magnetic field of 1 kOe applied parallel to the ribbons' quenched substrate velocity direction.

transition at the temperature of 630 K, which is in good agreement with the Curie temperature of $Sm_2Fe_{15}Ga_2C_2$ intermetallic compound [6], is attributed to the crystallized $Sm_2Fe_{15}Ga_2C_{2.2}$ (2:17) phase. 'Extra' magnetization detected at temperatures above 630 K results from the presence of α-Fe in these samples. The magnetic phase transition of α-Fe, however, is not observed in this temperature range due to its high Curie temperature ($T_C = 1043$ K). The temperature dependence of the magnetization demonstrates the presence of an elevated Curie temperature for the amorphous intergranular matrix adjacent to nanosized $Sm_2Fe_{15}Ga_2C_{2.2}$ and α-Fe crystallites. The difference in Curie temperature can probably be attributed to the following factors:

(1) differences in the Fe magnetic moment,
(2) composition differences, and
(3) molecular field penetration into the aip, which provides an 'extra' molecular field and extrinsically increases the Curie temperature.

These three factors are discussed separately.

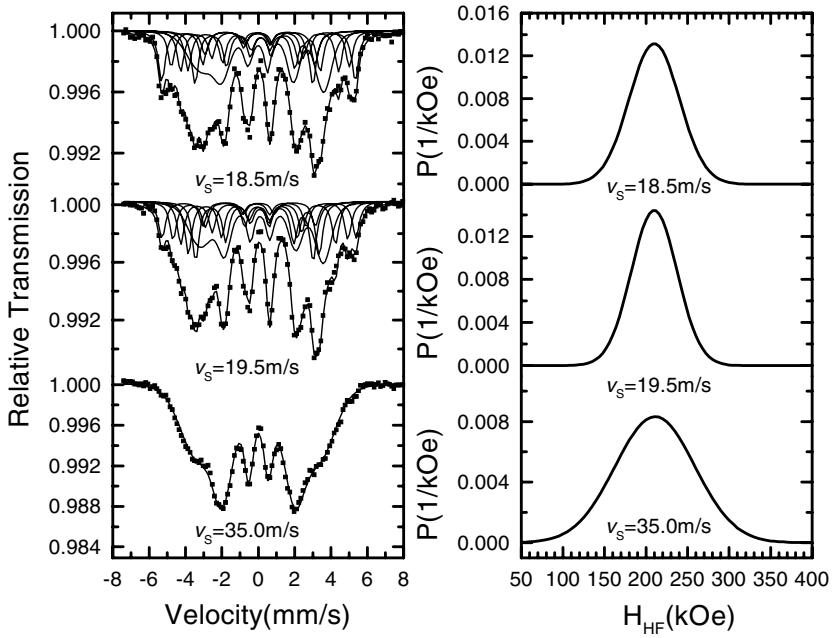

Figure 3. Room temperature ^{57}Fe Mössbauer spectra of as-quenched $Sm_2Fe_{18}Ga_2C_{2.2}$ samples prepared with different substrate velocities. In the right-hand panel of the figure the corresponding hyperfine field distributions used for fitting the amorphous phase are shown. The fitting procedure is described in the text.

It is difficult to determine the magnetic moments of Fe atoms in a multi-phase system by ordinary magnetization measurements. Mössbauer effect study, however, is a powerful technique for investigating the ^{57}Fe magnetic hyperfine field in each component, and hence we can obtain the magnetic moment of Fe on the basis of its relationship with the magnetic hyperfine field. Figure 3 illustrates room temperature ^{57}Fe Mössbauer spectra for as-quenched samples of $Sm_2Fe_{18}Ga_2C_{2.2}$ prepared at different substrate velocities. Two analysis models are proposed to fit the complex Mössbauer spectra. For crystalline magnetic phases, the Lorentzian multiplet analysis is suitable. This fitting model is a standard one that permits users to fit several Lorentzian singlets, doublets, or sextets, corresponding to paramagnetic sites with or without a quadrupole splitting and sites with a magnetic hyperfine field and a quadrupole splitting; for an amorphous state, the hyperfine parameters show a very broad distribution due to the lack of long-range order, and one should used the Voigt-based fitting analysis method because this model provides the means to obtain reliable distributions of hyperfine parameters. In the case of this model, the primary hyperfine parameter's distribution is represented by a sum of Gaussian components, enabling it to have nearly any shape. Secondary hyperfine parameters, such as the centre shift for paramagnetic generalized sites or the centre shift and quadrupole shift for magnetic generalized sites, can be linearly coupled to the primary hyperfine parameter. Therefore, for the samples quenched at 35.0 m s^{-1}, which contain only amorphous state, the spectrum can be fitted by the Voigt-based fitting analysis model. In the cases of the samples quenched at 18.5 and 19.5 m s^{-1}, which contain mixtures of crystalline and amorphous phases, a combination of Lorentzian multiplet analysis and Voigt-based fitting analysis models is used to fit the complex Mössbauer structure.

On the basis of the models proposed above, the fitting procedures for each component, i.e. α-Fe, $Sm_2Fe_{15}Ga_2C_{2.2}$, and the amorphous state, are described as follows.

Table 1. The amounts of different phases (in at.% Fe) and estimated composition of the aip in as-quenched $Sm_2Fe_{18}Ga_2C_{2.2}$ ribbons. T_c^a and T_c^{a*} are Curie temperature of the aip and the bulk amorphous alloy with the same composition as the aip, respectively.

v_s (m s^{-1})	α-Fe (at.% Fe)	$Sm_2Fe_{15}Ga2C_{2.2}$ (at.% Fe)	Amount (at.% Fe)	Estimated composition of the intergranular phase	T_c^a (K)	T_c^{a*} (K)
18.5	14.8 ± 2.0	33.1 ± 2.0	52.1 ± 4.0	$Sm_2Fe_{15.4\pm 0.5}Ga_2C_{2.2}$	498 ± 5	456 ± 5
19.5	10.6 ± 2.0	32.5 ± 2.0	56.9 ± 4.0	$Sm_2Fe_{16.2\pm0.5}Ga_2C_{2.2}$	497 ± 5	459 ± 5
35.0	0.0	0.0	100.0	$Sm_2Fe_{18.0}Ga_2C_{2.2}$	465 ± 5	465 ± 5

(1) Since no preferential orientation of the crystallites and no texture are observed from either x-ray diffraction or electron diffraction patterns, it is assumed that the magnetic grains are oriented isotropically to the γ-ray direction; the relative intensities for the six peaks of each sextet are fixed at 3:2:1:1:2:3.

(2) For the components of α-Fe, the magnetic hyperfine field of α-Fe is well known and fixed at 330 kOe. Since $Sm_2Fe_{15}Ga_2C_{2.2}$ magnetic crystalline phase with the Th_2Zn_{17}-type structure has four non-equivalent Fe sites, namely 6c, 9d, 18f, and 18h [6], and exhibits a uniaxial magnetocrystalline anisotropy [7], its spectrum can be fitted by four sextets of Lorentzian lines on the basis of Lorentzian multiplet models. As discussed by Zhou *et al* [8], the hyperfine fields for these four sextets decrease in the order 6c > 9d > 18f > 18h. It is well known that the relative absorbed area of each subspectrum is proportional to the number of Fe atoms at this site. On the basis of neutron diffraction results [9], the relative absorbed areas of the subspectra corresponding to 6c, 9d, 18f, and 18h sites are fixed to be proportional to the occupancy factors of Fe atoms at these four non-equivalent sites. The ^{57}Fe hyperfine fields corresponding to 6c, 9d, 18f, and 18h sites are 298 ± 4, 256 ± 4, 221 ± 4, and 196 ± 4 kOe, which are in good agreement with those for $Tb_2Fe_{15}Ga_2$ and $Sm_2Fe_{15}Ga_2$ [9, 10].

(3) For the component of the amorphous state, the spectrum is fitted with one sextet of Voigt lines corresponding to a very broad Gaussian hyperfine field distribution. The values of the average hyperfine field $\langle H \rangle$, average centre shift $\langle \mathrm{CS} \rangle$, and average quadrupole shift $\langle \varepsilon \rangle$ are 210 ± 2 kOe, 0.00 ± 0.02, and -0.02 ± 0.02 mm s^{-1}, respectively, and independent of the substrate velocity within the experimental error, implying that there is no difference in Fe magnetic moment between the aip and amorphous ribbon. However, the Gaussian width of the hyperfine field distribution decreases from 48 ± 2 kOe for the sample quenched at 35.0 m s^{-1} to 27 ± 5 kOe for the sample quenched at 19.5 m s^{-1}. The narrower hyperfine field distribution suggests that the atomic arrangement becomes more ordered in the aip compared with that in bulk amorphous materials.

On the basis of the relative areas of the various subspectra, the relative concentrations of different components (in at.% Fe) were obtained, and these are summarized in table 1. From x-ray diffraction patterns and Mössbauer spectra, we find that no cementite is formed during the preparation process. The composition of the aip can be estimated by subtracting the portions of crystallized Fe and $Sm_2Fe_{15}Ga_2C_{2.2}$ from the composition of the starting amorphous ribbon. The error bars of the proportions are about 2% and 4% for α-Fe and the aip, respectively, which corresponds to fluctuations in the atomic content of the intergranular phase of ± 0.5. The estimated Fe concentration in the aip is found to be definitely lower than that in amorphous ribbon quenched at 35.0 m s^{-1} (see table 1).

It is important to consider whether the enhancement of the Curie temperature originates from compositional differences. In order to answer this question, we prepared $Sm_2Fe_{15+x}Ga_2C_{2.2}$ ($x = 0.0$, 1.5, 3.0, and 4.5) amorphous ribbons at $v_s = 35.0$ m s^{-1} and

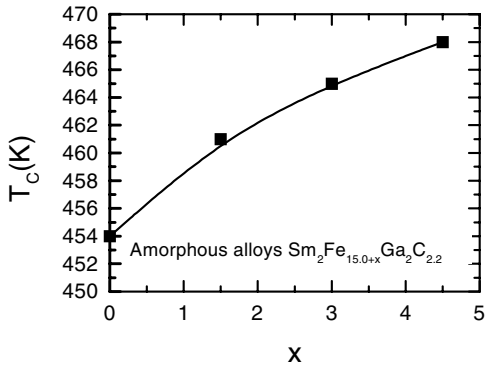

Figure 4. The compositional dependence of the Curie temperature measured for four amorphous Sm–Fe–Ga–C ribbons with excess iron content x.

investigated the effect of Fe concentration on the Curie temperature. As shown in figure 4, it is notable that the Curie temperatures of the amorphous ribbons decrease, rather than increase, with decreasing Fe concentration. Obviously, the enhancement of the Curie temperature for the aip cannot be attributed to differences in Fe concentration. The Curie temperature of the amorphous intergranular region is found to be about 42 and 38 K higher, for the samples quenched at 18.5 and 19.5 m s^{-1}, respectively, than for the fully amorphous ribbons of the same composition. This difference is much larger than the experimental errors in both the composition estimation and the measurement of the Curie temperature. Since we have excluded the possibility of differences in Fe magnetic moment and composition between the aip and bulk amorphous state, it can be concluded that the enhancement of the Curie temperature is due to the penetration of the molecular field of the crystallized magnetic phases into the amorphous intergranular region. A similar phenomenon has also been observed in the system of Fe–B–Nb–Cu nanocrystalline materials [11–13].

In recent work, Garcia and Hernando [14–16] have proposed that the molecular field does not vanish outside the ferromagnet but decreases exponentially with an effective length l of the order of the first-neighbour atomic distance. In the case where nanocrystallites are in contact with a ferromagnetic amorphous matrix, the molecular field of the crystallized ferromagnetic phase, H_m^{cr}, will penetrate into the aip. Therefore, the molecular field at a point x in the aip, $H_m^a(x)$, can be written as

$$H_m^a(x) = H_m^{a*} + (H_m^{cr} - H_m^{a*})\mathrm{e}^{-x/l} \qquad \text{for } 0 \leqslant x \leqslant \delta/2 \tag{1}$$

and

$$H_m^a(x) = H_m^{a*} + (H_m^{cr} - H_m^{a*})\mathrm{e}^{-(\delta-x)/l} \qquad \text{for } \delta/2 \leqslant x \leqslant \delta \tag{2}$$

where H_m^{a*} is the molecular field of bulk amorphous alloy with the same composition as the aip. δ is the width of the intergranular region, as illustrated in figure 5. The average molecular field in the amorphous matrix is given by

$$\overline{H_m^a} = H_m^{a*} + \frac{2l(H_m^{cr} - H_m^{a*})}{\delta}\int_0^{\delta/2} \mathrm{e}^{-x/l}\,\mathrm{d}x = H_m^{a*} + \frac{2l}{\delta}(H_m^{cr} - H_m^{a*})(1 - \mathrm{e}^{-\delta/2l}). \tag{3}$$

For Fe-rich compounds, the relationship between the Curie temperature and molecular field can be described as

$$k_B T_c = g\mu_0\mu_B H_m S \tag{4}$$

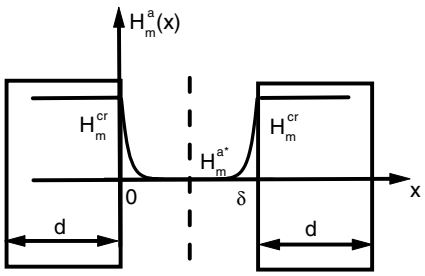

Figure 5. A schematic representation of the model used to calculate the Curie temperature enhancement due to the penetration of the molecular field from the ferromagnetic nanocrystallites (bold rectangular boxes) of diameter d and the amorphous phase in between. The explanation of the symbols is given in the text.

where k_B is the Boltzmann constant, μ_B is the Bohr magneton, g is the Landé g-factor of the Fe atoms, and S is the spin moment of Fe.

If we assume that the spin moments of the Fe atoms in the different phases are same, the Curie temperature of the aip T_c^a can be written as

$$T_c^a = T_c^{a*} + \frac{2l}{\delta}(T_c^{cr} - T_C^{a*})(1 - \mathrm{e}^{-\delta/2l}) \tag{5}$$

where T_c^{cr} is the Curie temperature of the crystallized ferromagnetic phase.

Since l is of the order of the first-neighbour distance (several ångströms) and $l \ll \delta$, i.e. $\mathrm{e}^{-\delta/2l} \cong 0$, T_c can be approximated as

$$T_c^a = T_c^{a*} + \frac{2l}{\delta}(T_c^{cr} - T_C^{a*}). \tag{6}$$

From this model, the maximum increase in T_c will be determined by the aip interacting entirely with α-Fe and the minimum by the aip in contact only with the crystalline alloy. From the data in figure 2, we see that the transition in the aip is complete by 500 K, so $\Delta T_{c,max} = 35$ K. Thus from equation (6), $\Delta T_{c,max} = \frac{2l}{\delta}(1043 - 465) = 35$. Hence we can obtain $\frac{2l}{\delta} \approx \frac{1}{17}$. Using this value for $\frac{2l}{\delta}$, one obtains $\Delta T_{c,min} = \frac{2l}{\delta}(630 - 465) \approx 10$ K. So the transition in the aip should straddle the temperature range 475–500 K, which appears to be consistent with the data in figure 2.

Acknowledgments

This work was supported by the State Key Project of Fundamental Research, the National Natural Sciences Foundation of China, as well as the Natural Sciences and Engineering Research Council of Canada. Z H Cheng thanks the Killam Foundation for financial support.

References

[1] Coehoorn R, de Mooij D B, Duchateau J P W B and Buschow K H J 1988 *J. Physique Coll.* **49** C8 669
[2] Manaf A, Buckley R A and Davies H A 1993 *J. Magn. Magn. Mater.* **128** 302
[3] Ding J, McCormick P G and Street R 1993 *J. Magn. Magn. Mater.* **124** L1
[4] Schrefl T, Fidler J and Kronmüller H 1994 *Phys. Rev.* B **49** 6100
[5] Cheng Z H, Zhang J X, Guo H Q, van Lier J, Kronmüller H and Shen B G 1998 *Appl. Phys. Lett.* **72** 1110
[6] Shen B G, Wang F W, Gong H Y, Cheng Z H, Liang B, Zhang J X and Zhang S Y 1995 *J. Phys.: Condens. Matter* **7** 883
[7] Buschow K H J 1991 *Rep. Prog. Phys.* **54** 1123

[8] Zhou R J, Rosenberg M, Katter M and Schultz L 1993 *J. Magn. Magn. Mater.* **118** 110
[9] Hu Z, Yelon W B, Mishra S, Long G J, Pringle O A, Middleton D P, Buschow K H J and Grandjean F G 1994 *J. Appl. Phys.* **76** 443
[10] Dunlap R A, MacKay G R and Wang Z 1997 *J. Alloys Compounds* **260** 28
[11] Hernando A, Navarro I and Gorria P 1995 *Phys. Rev.* B **51** 3281
[12] Lewis L H, Welch D O and Panchanathan V 1997 *J. Magn. Magn. Mater.* **175** 275
[13] Chen Z M, Daniil M, Hadjipanayis G C, Mounkarika A and Papaefthymiou V 1999 *J. Appl. Phys.* **86** 3857
[14] Garcia N and Hernando A 1991 *J. Magn. Magn. Mater.* **99** L12
[15] Hernando A, Navarro J, Prados C, Garcia D, Vazquez M and Alonso J 1996 *Phys. Rev.* B **53** 8223
[16] Hernando A, Navarro I, Prados C, Garcia D, Lesmes F, Freijo J J and Saledo A 1997 *Nanostruct. Mater.* **9** 459